

Verification of localized GRACE solutions by the Polish quasigeoid

Markus Antoni¹, Andrzej Borkowski², Wolfgang Keller¹, Magdalena Owczarek²

¹Institute of Geodesy, Stuttgart University

24D Geschwister-Scholl St., D-70174 Stuttgart, Germany

e-mail: markus.antoni@gis.uni-stuttgart.de; wolfgang.keller@gis.uni-stuttgart.de

²Institute of Geodesy and Geoinformatics, Wrocław University of

Environmental and Life Sciences

53 Grunwaldzka St., PL-50-357 Wrocław, Poland

e-mail: andrzej.borkowski@up.wroc.pl; magdalena.owczarek@up.wroc.pl

Received: 8 July 2009 / Accepted: 4 November 2009

Abstract: The GRACE-based model GGM02S is a global gravity model expressed in spherical harmonics. As the model is a global solution, a certain smoothing of the available gravity field information is unavoidable. For regional geoid determination the irregularities of residual gravity field should be included. The paper presents the global GRACE gravity field solution, regionally improved by adding a residual field, which is represented by radial base functions.

The GRACE observations over the territory of Poland are analysed and a regionally improved GRACE geoid from this data is derived. This improved regional geoid is compared with the Polish quasigeoid and differences between the global and regionally improved GRACE GGM02S solutions are discussed. The study shows that the error of the official GRACE GGM02s solution was reduced by 50% due to regional refinement.

Keywords: GRACE, quasigeoid, radial base function, line of sight gradiometry

1. Introduction

Global gravity field solutions obtained from GRACE K-band observations and expressed in spherical harmonics do not fully exploit the information contained in this data. As an example the original K-band data along an GRACE orbital arc crossing the Himalayan can be compared with the synthetic K-band data along the same arc, computed from a global GRACE solution for the same month. Figure 1 shows the difference between the original and the synthetic data and the topography beneath the arc. Recognizable, there is a correlation of the differences with the topography, meaning that the residual data consists not only of noise but still contains a signal, which is not represented by the global GRACE solution. Therefore, the GRACE gravity field solution can be improved regionally, by adding a residual field, which is represented by radial base functions. The location and shape of these radial base functions are to be estimated from the residual K-band data, i.e. from the difference between the original K-band data and the synthetic K-band data, computed from a global GRACE solution.

Unfortunately, the residual K-band data contains not only gravity field information but also errors coming from imperfect de-aliasing or calibration errors. Hence, an independent gravity field solution is necessary to discriminate in the regional solution between the gravity content and artefacts. For this purpose the Polish quasigeoid will be used, because of its homogeneity and high precision.

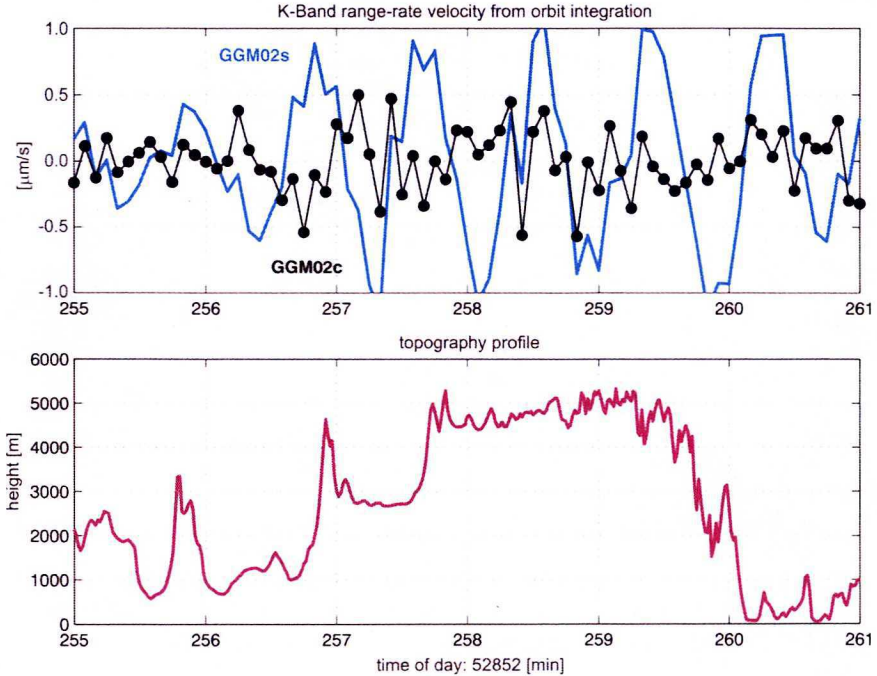


Fig. 1. Residual K-band observations along an arc over the Himalayan

2. Regional improvement of global GRACE solutions

The standard GRACE product is a gravity field model expressed in spherical harmonics. Because of the truncation of the spherical harmonics expansion at a certain degree and order N a certain smoothing of the available gravity field information is unavoidable. Wavelength shorter than $20\,000\text{ km}/N$ are simply not present in the solution. The resolution can only be enhanced, if the global solution is augmented by a correction field, represented by base functions with a finite supports or at least by rapidly decaying base functions. These functions modify the global solution only regionally, but contain all frequencies up to infinity. The simplest class of such rapidly decaying base functions are the so-called radial base functions. The class of radial base functions is characterized by the property that their values only depend on the spherical angle between their centre point $\boldsymbol{\eta}$ and the evaluation point $\boldsymbol{\xi}$. Let Ω be the unit sphere and $\sigma = \{\sigma_n\}$ be a sequence fulfilling the condition

$$\sum_{n \in \mathbb{N}} \frac{2}{2n+1} \sigma_n^2 < \infty \quad (1)$$

Then a radial base function on the unit sphere is a function of the following structure

$$\psi_{\boldsymbol{\eta}, \sigma}(\boldsymbol{\xi}) = \sum_{n \in \mathbb{N}} \left(\frac{1}{\|\boldsymbol{\xi}\|} \right)^{n+1} \sigma_n P_n \left(\left(\frac{\boldsymbol{\xi}}{\|\boldsymbol{\xi}\|} \right)^T \boldsymbol{\eta} \right), \quad \boldsymbol{\eta} \in \Omega, \quad \boldsymbol{\xi} \in \mathbb{R}^3 \setminus \Omega \quad (2)$$

Here, the functions P_n are the Legendre polynomials, the vector $\boldsymbol{\eta}$ points to the centre of the radial base function and the sequence $\{\sigma_n\}$ determines its shape. The function $\psi_{\boldsymbol{\eta}, \sigma}$ is harmonic outside Ω , radially symmetric around $\boldsymbol{\eta}$ and for a proper choice of the shape sequence $\{\sigma_n\}$ it rapidly decays with the distance between $\boldsymbol{\xi}/\|\boldsymbol{\xi}\|$ and $\boldsymbol{\eta}$.

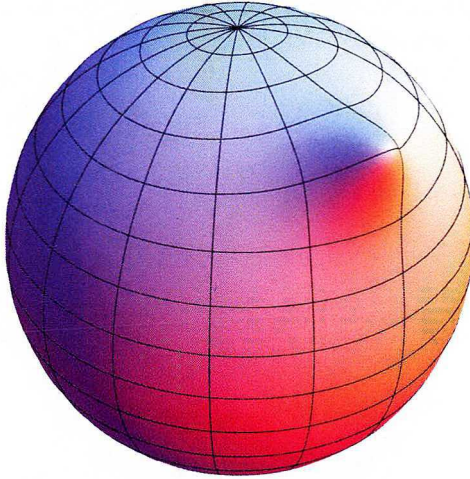


Fig. 2. Gravity field generated by a single radial base function

In Figure 2 a gravity field represented by a single radial base function $\psi_{\boldsymbol{\eta}, \sigma}$ located at $\boldsymbol{\eta}$ with the spherical coordinates $\boldsymbol{\eta} = \left(\frac{\pi}{4}, -\frac{\pi}{6} \right)$ is displayed. The intended regional improvement δV of the global GRACE solution is now to be constructed by the superposition of several radial base functions

$$\delta V(\boldsymbol{\xi}) = \sum_{i=1}^N c_i \psi_{\boldsymbol{\eta}_i, \sigma_i}(\boldsymbol{\xi}) \quad (3)$$

The scaling factors c_i , the position vectors $\boldsymbol{\eta}_i$ and the shape sequences σ_i have to be chosen in such a way that the regional improvement δV optimally fits the residual K-band data. Since only a finite number of residual K-band observations is available, it is impossible to determine the infinite real numbers of the shape sequences σ_i .

For this reason instead of the general shape sequences, only sequences generated by simple rules are taken into account and the parameters of the generating rules are estimated from the residual K-band data. One example of such a generating rule is

$$\sigma_n = \alpha^n, 0 < \alpha < 1 \quad (4)$$

With this choice $\psi_{\mathbf{\eta},\sigma}$ represents the potential of a unit point-mass located at $\alpha\mathbf{\eta}$. If for further use the choice of the shape sequence is restricted to the class described in (4), the notation of the radial base function can be changed into $\psi_{\mathbf{\eta},\alpha}$.

3. Line-of-sight gradiometry

In order to estimate the parameters c_i , $\mathbf{\eta}_i$, α_i of the regional improvement δV from residual K-band observations, a direct connection between these two items has to be established. In the experiments being presented here, this connection is generated in the form of the so called line-of-sight gradiometry (Keller and Sharifi, 2005). The idea of this approach will be sketched briefly now. The GRACE K-band observations can be expressed by the positions and the velocities of both satellites in the following way

$$\dot{\rho}(t) = \frac{(\dot{\mathbf{x}}_2(t) - \dot{\mathbf{x}}_1(t))^T(\mathbf{x}_2(t) - \mathbf{x}_1(t))}{\|\mathbf{x}_2(t) - \mathbf{x}_1(t)\|} \quad (5)$$

If the above equation is differentiated with respect to time, one obtains

$$\begin{aligned} \ddot{\rho}(t) = & \frac{(\ddot{\mathbf{x}}_2(t) - \ddot{\mathbf{x}}_1(t))^T(\mathbf{x}_2(t) - \mathbf{x}_1(t))\|\mathbf{x}_2(t) - \mathbf{x}_1(t)\|}{\|\mathbf{x}_2(t) - \mathbf{x}_1(t)\|^2} \\ & + \frac{\|\dot{\mathbf{x}}_2(t) - \dot{\mathbf{x}}_1(t)\|^2\|\mathbf{x}_2(t) - \mathbf{x}_1(t)\|}{\|\mathbf{x}_2(t) - \mathbf{x}_1(t)\|^2} \\ & - \frac{[(\dot{\mathbf{x}}_2(t) - \dot{\mathbf{x}}_1(t))^T(\mathbf{x}_2(t) - \mathbf{x}_1(t))]^2}{\|\mathbf{x}_2(t) - \mathbf{x}_1(t)\|^3} \end{aligned}$$

Using the Newtonian equation of motion

$$\ddot{\mathbf{x}}(t) = \nabla V(\mathbf{x}(t)) \quad (6)$$

the difference in the accelerations of both satellites can be expressed as the second order derivative of the potential in flight-direction of the satellites

$$\ddot{\mathbf{x}}_2(t) - \ddot{\mathbf{x}}_1(t) = \nabla V(\mathbf{x}_2(t)) - \nabla V(\mathbf{x}_1(t)) \quad (7)$$

$$\ddot{\mathbf{x}}_2(t) - \ddot{\mathbf{x}}_1(t) = \nabla^2 V \left(\frac{\mathbf{x}_2(t) - \mathbf{x}_1(t)}{2} \right) (\mathbf{x}_2(t) - \mathbf{x}_1(t)) + O((\mathbf{x}_2(t) - \mathbf{x}_1(t))^2) \quad (8)$$

If the second order derivative of the potential in flight-direction is denoted by Γ

$$\Gamma = \frac{(\mathbf{x}_2(t) - \mathbf{x}_1(t))^T}{\|\mathbf{x}_2(t) - \mathbf{x}_1(t)\|} \nabla^2 V \left(\frac{\mathbf{x}_2(t) - \mathbf{x}_1(t)}{2} \right) \frac{(\mathbf{x}_2(t) - \mathbf{x}_1(t))}{\|(\mathbf{x}_2(t) - \mathbf{x}_1(t))\|} \quad (9)$$

this gravity gradient can be computed from the range acceleration by

$$\begin{aligned} \Gamma &= \frac{\ddot{\rho}(t)}{\|\mathbf{x}_2(t) - \mathbf{x}_1(t)\|} \\ &\quad - \frac{\|\dot{\mathbf{x}}_2(t) - \dot{\mathbf{x}}_1(t)\|^2 \|\mathbf{x}_2(t) - \mathbf{x}_1(t)\|}{\|\mathbf{x}_2(t) - \mathbf{x}_1(t)\|^3} \\ &\quad + \frac{[(\dot{\mathbf{x}}_2(t) - \dot{\mathbf{x}}_1(t))^T (\mathbf{x}_2(t) - \mathbf{x}_1(t))]^2}{\|\mathbf{x}_2(t) - \mathbf{x}_1(t)\|^4} \\ &= \frac{\ddot{\rho}}{\rho} - \frac{\|\Delta \dot{\mathbf{x}}\|}{\rho^2} + \frac{\dot{\rho}^2}{\rho^2} \end{aligned}$$

which exactly corresponds to formula (3) in (Keller and Sharifi, 2005). The last two terms in the expression above are correction terms and can be computed from the approximate positions and velocities $\mathbf{x}_i^{(0)}, \dot{\mathbf{x}}_i^{(0)}$; $i = 1, 2$ of the two satellites, obtained from a numerical orbit integration in a reference field:

$$\begin{aligned} \Gamma &= \frac{\ddot{\rho}(t)}{\|\mathbf{x}_2(t) - \mathbf{x}_1(t)\|} \\ &\quad - \frac{\|\dot{\mathbf{x}}_2^{(0)}(t) - \dot{\mathbf{x}}_1^{(0)}(t)\|^2 \|\mathbf{x}_2^{(0)}(t) - \mathbf{x}_1^{(0)}(t)\|}{\|\mathbf{x}_2^{(0)}(t) - \mathbf{x}_1^{(0)}(t)\|^3} \\ &\quad + \frac{[(\dot{\mathbf{x}}_2^{(0)}(t) - \dot{\mathbf{x}}_1^{(0)}(t))^T (\mathbf{x}_2^{(0)}(t) - \mathbf{x}_1^{(0)}(t))]^2}{\|\mathbf{x}_2^{(0)}(t) - \mathbf{x}_1^{(0)}(t)\|^4} \end{aligned} \quad (10)$$

Hence, after pre-processing of the K-band data according to (10), the line-of-sight gravity gradients at the barycenter of the two satellites are available. Splitting up the unknown potential V into its known reference part V_0 and its unknown correction part δV , results in the following observation equation:

$$\begin{aligned} \delta\Gamma &= \Gamma - \frac{(\mathbf{x}_2(t) - \mathbf{x}_1(t))^T}{\|\mathbf{x}_2(t) - \mathbf{x}_1(t)\|} \nabla^2 V_0 \left(\frac{\mathbf{x}_2(t) - \mathbf{x}_1(t)}{2} \right) \frac{(\mathbf{x}_2(t) - \mathbf{x}_1(t))}{\|\mathbf{x}_2(t) - \mathbf{x}_1(t)\|} \\ &= \frac{(\mathbf{x}_2(t) - \mathbf{x}_1(t))^T}{\|\mathbf{x}_2(t) - \mathbf{x}_1(t)\|} \nabla^2 \delta V \left(\frac{\mathbf{x}_2(t) - \mathbf{x}_1(t)}{2} \right) \frac{(\mathbf{x}_2(t) - \mathbf{x}_1(t))}{\|\mathbf{x}_2(t) - \mathbf{x}_1(t)\|} \\ &= \sum_{i=1}^N c_i \frac{(\mathbf{x}_2(t) - \mathbf{x}_1(t))^T}{\|\mathbf{x}_2(t) - \mathbf{x}_1(t)\|} \nabla^2 \psi_{\mathbf{n}_i, \alpha_i} \left(\frac{\mathbf{x}_2(t) - \mathbf{x}_1(t)}{2} \right) \frac{(\mathbf{x}_2(t) - \mathbf{x}_1(t))}{\|\mathbf{x}_2(t) - \mathbf{x}_1(t)\|} \end{aligned} \quad (11)$$

This is a non-linear observation equation for the unknown parameter $\boldsymbol{\eta}_i$, α_i , $i = 1, 2, \dots, N$. In the c_i the observation equation is linear. For this reason methods of non-linear optimisation have to be applied for the estimation of these parameters.

4. Unconstrained minimization

In the following we will investigate the non-linear least squares problem

$$\|F(\mathbf{x})\|^2 \rightarrow \min \quad \text{for } F : \mathfrak{X}^n \rightarrow \mathfrak{X}^m, \quad m > n \quad (12)$$

The observation equation (10) can be brought into the normal form (12) by setting

$$\mathbf{x}^T = (c_1, \dots, c_N, \alpha_1, \dots, \alpha_N, \boldsymbol{\eta}_1, \dots, \boldsymbol{\eta}_N) \quad (13)$$

and

$$F_j(\mathbf{x}) = \delta\Gamma(t_j) - \sum_{i=1}^N c_i \frac{(\mathbf{x}_2(t_j) - \mathbf{x}_1(t_j))^T}{\|\mathbf{x}_2(t_j) - \mathbf{x}_1(t_j)\|} \nabla^2 \psi_{\boldsymbol{\eta}_i, \alpha_i} \left(\frac{\mathbf{x}_2(t_j) - \mathbf{x}_1(t_j)}{2} \right) \frac{(\mathbf{x}_2(t_j) - \mathbf{x}_1(t_j))}{\|\mathbf{x}_2(t_j) - \mathbf{x}_1(t_j)\|} \quad (14)$$

$$j = 1, 2, \dots, m$$

The idea is that starting from an initial guess \mathbf{x}_0 in each iteration step k an improved guess \mathbf{x}_{k+1} is computed in such a way that the sequence of target-function values $\|F(\mathbf{x}_k)\|^2$ is monotonously falling. In other words, in each step the misfit between $\mathbf{0}$ and $F(\mathbf{x}_k)$ has to be reduced. This can be achieved by approximating F linearly in \mathbf{x}_k

$$F(\mathbf{x}) \approx F(\mathbf{x}_k) + \nabla F(\mathbf{x}_k)(\mathbf{x} - \mathbf{x}_k) \quad (15)$$

and determining \mathbf{x} in such a way, that the linear approximation becomes $\mathbf{0}$. This leads to the iteration

$$\mathbf{x}_{k+1} = \mathbf{x}_k - (\nabla F(\mathbf{x}_k)^T \nabla F(\mathbf{x}_k))^{-1} \nabla F(\mathbf{x}_k)^T F(\mathbf{x}_k) \quad (16)$$

In the mathematical literature the iteration (14) is known as Gauss-Newton iteration (Ortega and Rheinboldt, 1970). In practical applications the Gauss-Newton iteration is lacking a certain robustness. This means, close to a local minimum the Jacobian $\nabla F(\mathbf{x}_k)$ gets almost rank-deficient and numerical rounding errors can degrade the solution of the normal equations

$$(\nabla F(\mathbf{x}_k)^T \nabla F(\mathbf{x}_k))(\mathbf{x} - \mathbf{x}_k) = \nabla F(\mathbf{x}_k)^T F(\mathbf{x}_k) \quad (17)$$

considerably. For this reason a regularization is necessary. This can be achieved by requiring that the step-length is below a certain bound

$$\|\mathbf{x} - \mathbf{x}_k\| < r_k \quad (18)$$

The bounds r_k are chosen so, that the sequence of target-function values is indeed decreasing. The regularized version of the Gauss-Newton method is known as Levenberg-Marquardt method or as trust-region method (Marquardt, 1963). Well tested implementations of the Levenberg-Marquardt algorithm are available both as public-domain software as well as toolboxes of commercial products.

For regional gravity improvement the Levenberg-Marquardt method was successfully applied in Antoni et al. (2008) and Antoni et al. (2009), using the energy-balance as observation type. As the energy-balance provides only a rather coarse resolution, for the quasigeoid improvement the line-of-sight gradiometry will be used instead.

5. Penalty methods

If an unconstrained minimization technique as for instance the Levenberg-Marquardt iteration is applied to the problem (10), the initial guess for the parameters $\boldsymbol{\eta}_i$, α_i , $i = 1, 2, \dots, N$ comes from prior information or from geophysical estimations. During the iteration process these parameters can move arbitrarily far from the initial guess and can end up with values, which are geophysically not reasonable. In order to avoid this, constraints

$$|\alpha_i - \alpha_{i,0}| < \Delta\alpha, \quad \|\boldsymbol{\eta}_i - \boldsymbol{\eta}_{i,0}\| < \Delta\boldsymbol{\eta} \quad (19)$$

have to be added. These constraints are implemented as so-called penalty functions (Courant, 1943)

$$\varphi_\alpha(\alpha_i) = \begin{cases} 0 & , |\alpha_i - \alpha_{i,0}| < \Delta\alpha \\ e^{\mu(\alpha_i - \alpha_{i,0})^2} & , \text{else} \end{cases} \quad (20)$$

and

$$\varphi_{\boldsymbol{\eta}}(\boldsymbol{\eta}_i) = \begin{cases} 0 & , \|\boldsymbol{\eta}_i - \boldsymbol{\eta}_{i,0}\| < \Delta\boldsymbol{\eta} \\ e^{\mu\|\boldsymbol{\eta}_i - \boldsymbol{\eta}_{i,0}\|^2} & , \text{else} \end{cases} \quad (21)$$

This means, no penalty has to be paid, if a parameter is inside the assigned bounds and the penalty grows exponentially if it moves out of these bounds. Hence, the new non-linear least-squares problem is

$$\|G(\mathbf{x})\|^2 \rightarrow \min \text{ for } G : \mathfrak{R}^n \rightarrow \mathfrak{R}^{m+k} \quad (22)$$

with

$$G(\mathbf{x}) = (F_1(\mathbf{x}), \dots, F_m(\mathbf{x}), \varphi_\alpha(\alpha_1), \dots, \varphi_\alpha(\alpha_N), \varphi_{\boldsymbol{\eta}}(\boldsymbol{\eta}_1), \dots, \varphi_{\boldsymbol{\eta}}(\boldsymbol{\eta}_N))^T \quad (23)$$

This augmentation by penalty functions enables to solve the constrained non-linear problem by minimization techniques.

6. The Polish quasigeoid model

The quasigeoid model used for verification of the obtained results is the model named “quasigeoid 2001”. This is a generally accessible quasigeoid model for Poland, recommended by The Head Office for Geodesy and Cartography in Poland as a standard for densification of vertical control with GPS.

The “quasigeoid 2001” model was determined by fitting the gravimetric quasigeoid model quasi97b to height anomalies at the sites of Polish GPS/levelling networks (Pażus et al., 2002).

The determination of the quasigeoid model quasi97b was based on the $1' \times 1'$ grid of free-air gravity anomalies, generated from available gravity data for territory of Poland and neighbouring countries (Łyszkowicz, 2002). The quasigeoid model was developed by the remove-restore technique, using the Fast Fourier Transform, where the global effects were represented by the geopotential model EGM96. The accuracy of this model was estimated at the level of 5 cm.

The available data from GPS/levelling points were GPS-derived heights and normal heights referred to Kronstadt86 at the 752 sites of the following Polish GPS/levelling networks:

- EUREF-POL – the extension of the European Reference Frame in the territory of Poland,
- POLREF – densification of EUREF-POL network,
- EUVN – Polish part of European Vertical GPS-Reference Network,
- WSSG – Military Satellite Geodetic Network, established for the automatic navigation purposes,
- TATRY – the network established by the Institute of Geodesy and Cartography in Tatra Mountains.

Quasi97b model was fitted to the GPS/levelling quasigeoid at the points of the above networks with the use of third degree polynomial and thin plate spline function.

Since the “quasigeoid 2001” model was developed, newer gravity data, geopotential models and development of high-resolution digital terrain models stimulated extensive research on Polish quasigeoid modelling. The recent research on the determination of precise quasigeoid in Poland had been conducted in 2002-2005 within the framework of the project “Determination of a centimetre geoid model in Poland with the use of geodetic data, gravity data, astronomical data, geological data and satellite data” supported by the Polish Committee for Scientific Research (Kryński and Łyszkowicz, 2006a). As a result, there was a number of new quasigeoid models developed: an astro-gravimetric model, gravimetric quasigeoid models, GPS/levelling models, an integrated model and the best-fitted model. An overview and summarization of this models is given by Kryński and Łyszkowicz (2006b).

For the verification of localized GRACE solutions the “quasigeoid 2001” was used because of the common access of the model. Moreover the accuracy of the model is sufficient for that purpose. Based on the “quasigeoid 2001” a dense grid of quasigeoid heights was interpolated. The short- and long- wavelength featured difference between

quasigeoid and geoid is insignificant for the purpose of validation of regional gravity field improvement discussed in this paper.

7. Numerical experiments

7.1. Closed loop simulation of regional gravity improvement using line-of-sight gradiometry

The first step in the conducted numerical experiments is the verification of the algorithm described above by a simulation study. For this purpose the EGM96 model, complete up to degree and order 60 was chosen as reference field V_0 . The residual field δV was generated by the superposition of 20 radial base functions $\psi_{\mathbf{n}_i, \alpha_i}$, where the location parameters \mathbf{n}_i were randomly chosen within Middle-Europe and the shape parameters were also randomly chosen within the interval $[0.9, 0.999]$. The closed-loop simulation consisted of 8 steps:

1. Within the combined field $V = V_0 + \delta V$ the one-month orbits of the two GRACE satellites were numerically integrated.
 2. From the integrated positions and velocities $\mathbf{x}_i(t), \dot{\mathbf{x}}_i(t), i = 1, 2$ the range rates $\dot{\rho}(t)$ were derived.
 3. The range rates $\dot{\rho}(t)$ were converted line-of-sight gradients Γ .
 4. These three steps were repeated for the reference field V_0 only, delivering the reference line-of-sight gradients Γ_0 .
 5. The residual line-of-sight gradients $\delta\Gamma = \Gamma - \Gamma_0$ were computed.
 6. The non-linear least squares problem (14) was solved by Levenberg-Marquardt iteration, leading to an estimation $\widehat{\delta V}$ of the residual potential δV .
 7. Steps 1 to 5 were repeated for $\hat{V} = V_0 + \widehat{\delta V}$ leading to estimated residual line-of-sight gradients $\widehat{\delta\Gamma}$.
- $\widehat{\delta V}$ was compared to δV and $\widehat{\delta\Gamma}$ was compared to $\delta\Gamma$.

The flow-chart of the closed-loop simulation study is given in Figure 3. The residual line-of-sight gradients $\delta\Gamma$, where the non-linear least-squares adjustment starts from, their estimation $\widehat{\delta\Gamma}$ after non-linear least-squares adjustment and the difference between both fields are displayed in Figure 4. Visually, it is hard to distinguish between the real residual line-of-sight gradients $\delta\Gamma$ and the estimated line-of-sight gradients $\widehat{\delta\Gamma}$. Their difference amounts only to about 30% of the given signal. The difference between the given and the estimated residual gradients has two sources:

The simulated noise in the data propagates into the estimated parameters.

The initial guess is not made manually but automatically by the algorithm. Therefore, the number of base functions used for the non-linear least-squares adjustment does not necessarily coincide with the number of base functions used for the generation of the residual field.

Another view onto the results are the histograms of the given gradients, the estimated gradients and the histogram of the differences between them. These histograms

are displayed in Figure 5. The figure shows that both the histogram of the given and of the estimated data is non-symmetric. This means, the data contains not only noise but also a weak signal. The histogram of the difference almost resembles the probability density of the normal distribution. One can conclude that the non-linear least-squares adjustment extracts most of the weak signal from the data and leaves only a normal distributed noise.

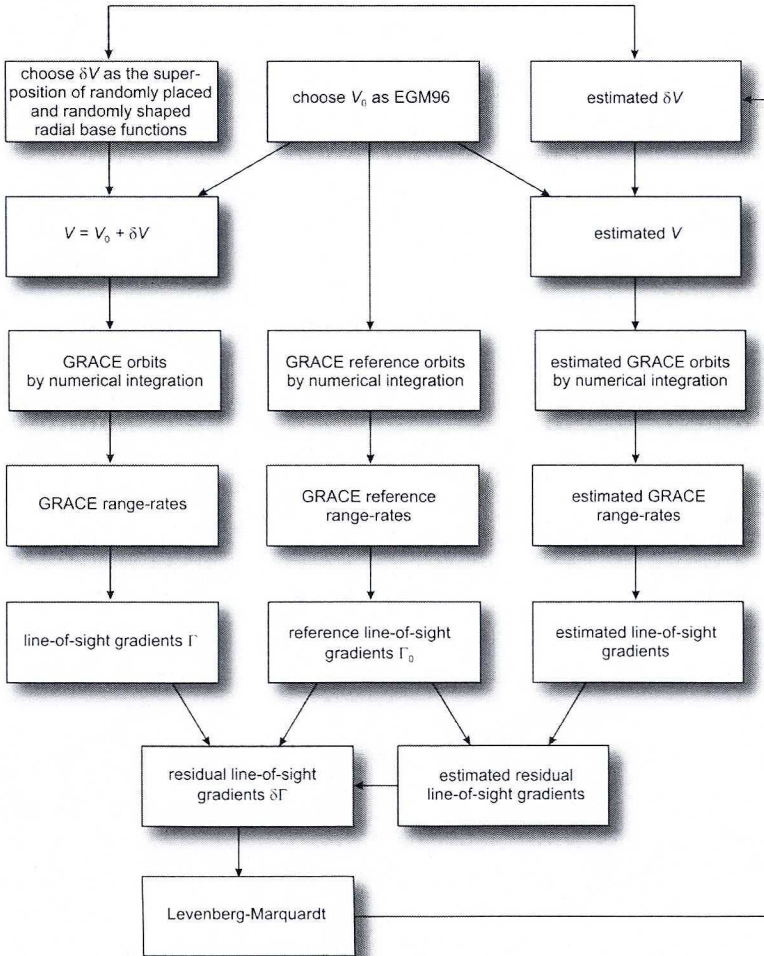


Fig. 3. Flow-chart of closed-loop simulation of regional gravity improvement using line-of-sight gradiometry

All in all it seems to be justified to say that the non-linear least-squares algorithm for regional gravity field improvement works properly, at least as long as the gravity field information in the residual data is not too strongly overpowered by non-gravitative error sources.

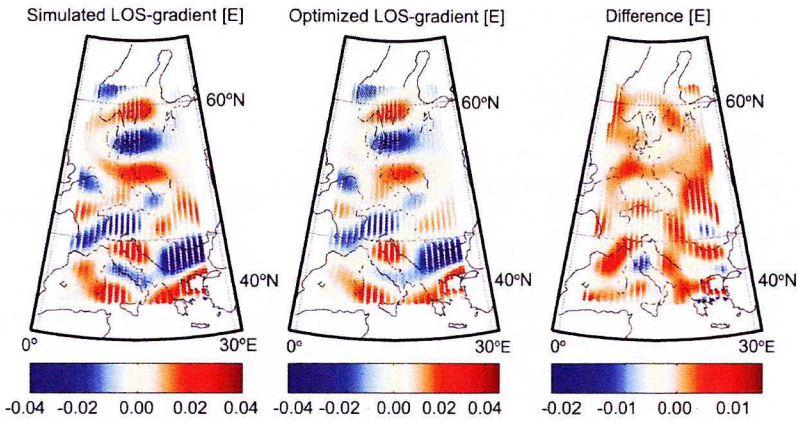


Fig. 4. Results of the simulation study

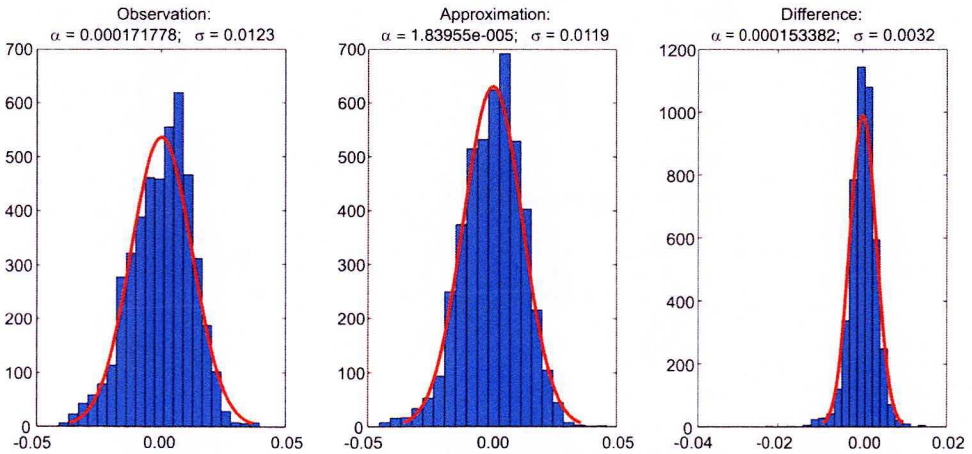


Fig. 5. Histograms of the given data, the estimated data and their difference

7.2. Verification of the non-linear least-squares GRACE solution by the Polish quasigeoid

After gaining confidence into the usability of the non-linear algorithm for gravity field improvement using residual GRACE data, the algorithm has to be validated by real data. Only a completely independent data source can be used for such a validation. The “quasigeoid 2001” model for Poland was chosen for such a validation, due to its excellent quality and homogeneity. Figure 6 explains the initial situation.

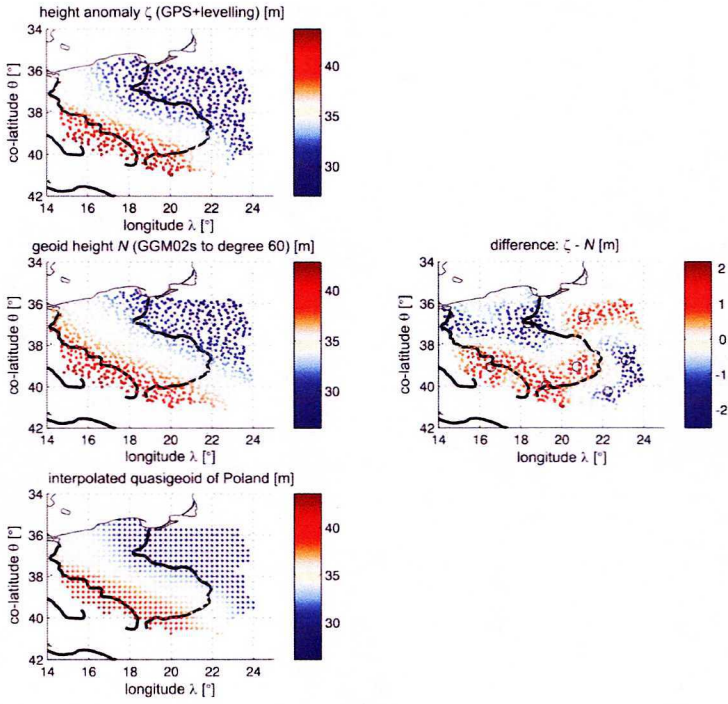


Fig. 6. Initial situation for the validation

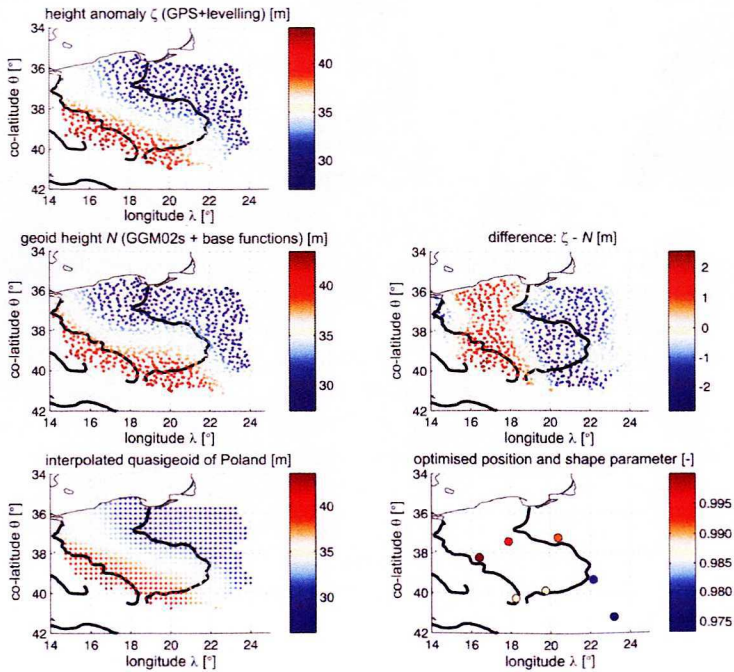


Fig. 7. One month regional improvement of global GRACE solution

The images in the left column show different solutions for the Polish quasigeoid. The top image is the quasigeoid model, the middle image the geoid computed from the GRACE GGM02s model (Tapley et al., 2005) complete up to degree and order 60, and the bottom image is the quasigeoid solution from an integrated gravity-GPS-levelling quasigeoid. In the right column the difference between the quasigeoid and the GRACE geoid is displayed. It is visible that the global GRACE solution is only a coarse approximation of the quasigeoid. Not only that the difference between them amounts up to 2 m, also details are missing in the global GRACE solution. For instance, the 35 m geoid undulation band running from south-west to north-east is almost a straight line in the GRACE solution, while it shows a significant curvature both in the quasigeoid as well as in the integrated gravity-GPS-levelling quasigeoid. Figure 7 shows the change of the situation when additional GRACE data from May 2003 was used to improve the global GRACE solution regionally. The arrangement of images in Figure 7 is basically the same as in Figure 6.

Only the global GRACE GGM02s solution is replaced by the regionally improved solution. In the right column an additional image was added, showing the estimated positions and the shape parameters of the radial base functions. The figure shows that the difference between the regionally improved GRACE solution and the quasigeoid dropped down from 2 m to only 1 m. Also the 35 m geoid undulation band now shows more structure than before. Amazingly, this considerable improvement was possible using only one month of data and only 7 base functions. For a further improvement the estimated residual line-of-sight gradients $\widehat{\delta\Gamma}$ are used as new input data and are analysed in the same way as the original residual line-of-sight gradients $\delta\Gamma$, giving second order estimations $\widehat{\delta V_1}$ for the residual potential and for the residual line-of-sight gradients $\widehat{\delta\Gamma_1}$. The combined gravity field solution is thus $\hat{V} = V_0 + \widehat{\delta V} + \widehat{\delta V_1}$. The combined solution is compared to the Polish quasigeoid in Figure 8. Visually, there is no difference between the solution given in Figure 7 and the combination solution displayed in Figure 8.

A more detailed picture gives the error statistics. In Figure 9 mean value, rms, maximum and minimum of the differences between the Polish quasigeoid and geoid from regionally improved GRACE solution are displayed. The blue columns refer to the one-step solution and the yellow columns refer to the combined solution. The combined solution does not differ much from the one-step solution. Only the rms became a little smaller. This means that the second step could not do more than only smooth the solution slightly. The reason for that can be explained by Figure 5. The residual line-of-sight gradients $\widehat{\delta\Gamma}$ have an almost perfect normal distribution density histogram. This means that $\widehat{\delta\Gamma}$ contains practically no gravity information but only errors of different sources.

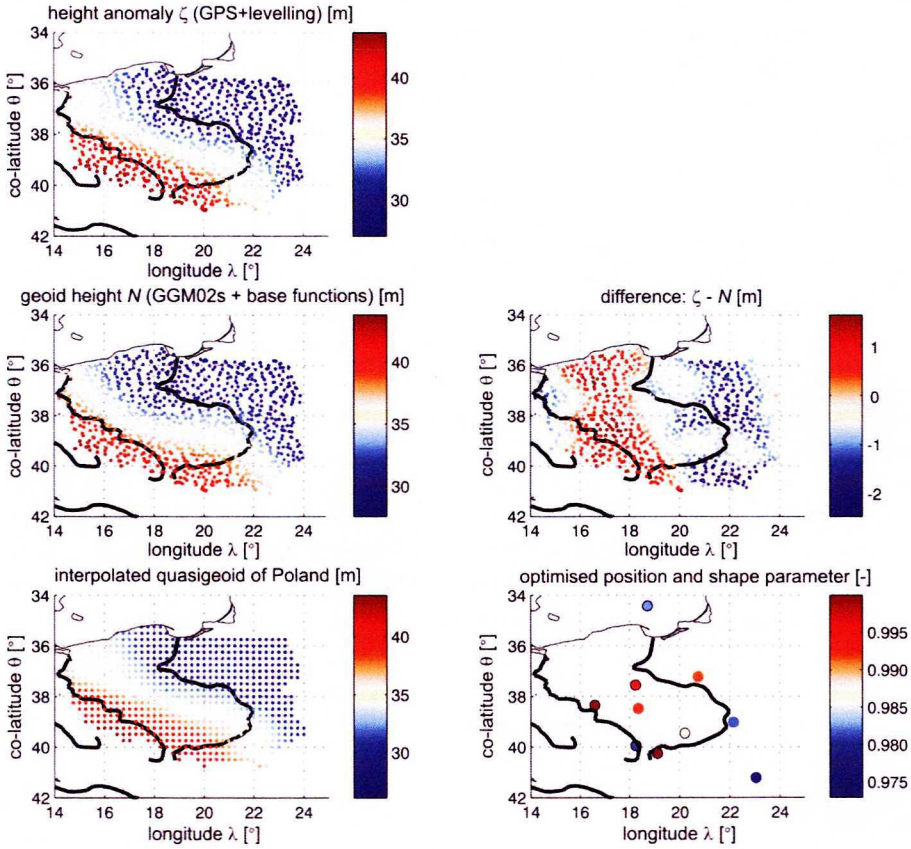


Fig. 8. Combination solution

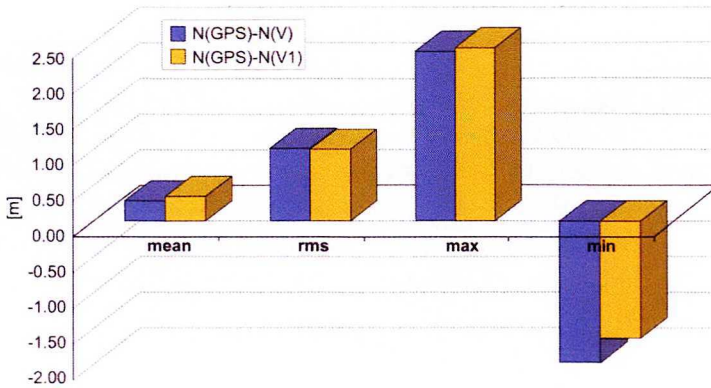


Fig. 9. Statistics of the differences of the one-step solution $N(\text{GPS})-N(V)$ and the combined solution $N(\text{GPS})-N(V1)$ to the quasigeoid

8. Conclusions

In the article a method was presented to improve global GRACE solution regionally, using radial base function for the refined analysis. The method was tested in a closed-loop simulation and against the Polish quasigeoid. The simulation study proved that the method basically gives the correct answer, limited only by the errors contained in the data and the quality of the initial guess.

The application of the method to GRACE data of May 2003, reduced the error of the official GRACE GGM02s solution by 50%, while the remaining error is around 1 m. This error can be attributed to the limited resolution of the GRACE missions. The size of the Polish territory is just at the resolution limit of this mission.

A further improvement will be possible using data of the recently launched GOCE mission instead of GRACE data. GOCE will provide an up to four times higher resolution as GRACE. Even more, the original data types of the GOCE mission are already gravity gradients. Hence, the presented method is well prepared for the processing of GOCE data. The GOCE observation can be used directly and it is not longer necessary to convert the original observations into gravity gradients, as it was necessary for GRACE data. This obsolete pre-processing step, will further increase the performance of the method presented here.

Acknowledgments

This research was done with the financial support of the Ministry of Sciences and Higher Education, Poland and the German Academic Exchange Service within the framework of research project "Interpolation of the Polish Levelling Quasigeoid Using GOCE Data".

References

- Antoni M., Keller W., Weigelt M., (2008): *Regionale Schwerefeldmodellierung durch Slepian- und radiale Basisfunktionen*, ZfV, 133, pp. 120-129.
- Courant R., (1943): *Variational methods for the solution of problems of equilibrium and vibrations*, Bull. Amer. Math. Soc., 49, pp. 1-23.
- Keller W., Sharifi M., (2005): *Satellite gradiometry using a satellite pair*, Journal of Geodesy, Vol. 78, pp. 544-557.
- Krynski J., Łyszkowicz A., (2006a): *Regional quasi-geoid determination in the area of Poland*, In 5th FIG Regional Conference for Africa, Accra, Ghana, 8 - 11 March 2006.
- Kryński J., Łyszkowicz A., (2006b): *The overview of precise quasigeoid modelling in Poland*, 2nd Workshop on International Gravity Field Research, 8 - 9 May, Smolenice, Slovakia, Contributions to Geophysics and Geodesy, Special issue, WIGFR 2006, Geophysical Institute of Slovak Academy of Sciences, pp. 113-149.
- Łyszkowicz A., (2002): *The analysis of the gravity field data in view of the subdecimetre geoid in Poland*, In Proceedings of the 3rd Meeting of the International Gravity and Geoid Commission Gravity and Geoid 2002, 26 - 30 August 2002, Thessaloniki, Greece.

- Marquardt D., (1963): *An algorithm for least-squares estimation of non-linear parameters*, J. Appl. Math., 11, pp. 431-441.
- Ortega J., Rheinboldt W., (1970): *Iterative Solution of Nonlinear Equations in Several Variables*, Academic Press, New York.
- Pazus R., Osada E., Olejnik S., (2002): *Geoida niwelacyjna 2001*, Magazyn Geoinformacyjny Geodeta, 84, pp. 10-17.
- Tapley B., Ries J., Bettadpur S., Chambers D., Cheng M., Condi F., Gunter B., Kang Z., Nagel P., Pastor R., Pekker T., Poole S., Wang F., (2005): *GGM02-An improved Earth gravity field model from GRACE*, Journal of Geodesy, Vol. 79, pp. 467-478.
- Weigelt M., Antoni M., Keller W., (2009): *Regional gravity recovery from grace using position-optimized radial base functions*, In Proceedings of the IAG International Symposium on Gravity, Geoid and Earth Observations GGEO 2008, Chania, Crete, 23 - 27 June 2008, pp. 203-299.

Weryfikacja lokalnych rozwiązań GRACE za pomocą modelu quasigeoidy dla Polski

Markus Antoni¹, Andrzej Borkowski², Wolfgang Keller¹, Magdalena Owczarek²

¹Institut Geodezji, Uniwersytet w Stuttgarcie
ul. Geschwister-Scholl 24D, D-70174 Stuttgart

e-mail: markus.antoni@gis.uni-stuttgart.de; wolfgang.keller@gis.uni-stuttgart.de

²Institut Geodezji i Geoinformatyki, Uniwersytet Przyrodniczy we Wrocławiu
ul. Grunwaldzka 53, PL-50-357 Wrocław

e-mail: andrzej.borkowski@up.wroc.pl; magdalena.owczarek@up.wroc.pl

Streszczenie

Model GGM02S wyznaczony na podstawie danych z misji GRACE jest globalnym modelem grawimetrycznym opartym na harmonikach sferycznych. Ponieważ model ten jest globalnym rozwiązaniem, nieuniknione jest pewne wygładzenie informacji grawimetrycznych. Dla wyznaczenia lokalnego modelu geoidy konieczne jest uwzględnienie informacji o zmienności lokalnego pola grawitacyjnego. W pracy przedstawiono globalne rozwiązanie GRACE, poprawione przez dodanie informacji o lokalnym polu grawitacyjnym, określonym za pomocą radialnych funkcji bazowych. Obserwacje GRACE z obszaru Polski zostały przeanalizowane i na ich podstawie został wyznaczony ulepszony lokalny model geoidy. Model ten porównano z istniejącym modelem quasigeoidy dla Polski „quasigeoida 2001”, oraz przeanalizowano różnice uzyskane pomiędzy globalnym a lokalnie wzmocnionym rozwiązaniem GRACE GGM02S. Badania wykazały, że zastosowanie modelowania regionalnego zmniejsza o 50% błąd oficjalnego rozwiązania GRACE GGM02S.